Preprints of the 21st IFAC World Congress (Virtual)
Berlin, Germany, July 12-17, 2020

Support vector machine for a diesel engine performance and NO_x emission control-oriented model

Masoud Aliramezani * **Armin Norouzi** * **Charles Robert Koch** *

* *Mechanical Engineering Department, University of Alberta (e-mail: aliramez@ualberta.ca, norouziy@ualberta.ca, bob.koch@ualberta.ca)*

Abstract: A control oriented diesel engine NO_x emission and Break Mean Effective Pressure (BMEP) model is developed using Support Vector Machine (SVM). Steady state experimental data from a medium duty diesel engine is used to develop BMEP and NO_x emission model using Support Vector Machine (SVM). The engine speed, the amount of injected fuel and the injection rail pressure are used as input variables to predict the steady state engine NO_x emission and BMEP. The steady state model results were then implemented in the control oriented model. A fast response electrochemical NO_x sensor is used to experimentally study the engine transient NO_x emission and to verify the transient response of the control oriented model. The results show that the SVM algorithm is capable of accurately learning the engine BMEP and NO_x which improves the accuracy of the control oriented model compared to a conventional regression algorithm (trust-region) used in the literature. The control oriented model results closely match the experiments in both transient and steady state conditions with a root mean square error of 0.26 (bar) and 10 (ppm) for BMEP and NO_x respectively.

Keywords: Control Oriented Mode; Machine Learning; Support Vector Machine (SVM); Diesel engine; Emissions;

1 Introduction

Compression ignition (CI) engines are widely used in transportation (Dhar and Agarwal, 2014; Yadav et al., 2016), power generation (Dasappa and Sridhar, 2013), combined heat and power generation (CHP) (Bari and Hossain, 2013), agriculture (Pali et al., 2015) and many other applications due to their high thermal efficiency (Tan et al., 2017) and their long lifespan (Pronk et al., 2009). However, reducing the engine emissions to meet the stringent emission regulations has always been an ongoing challenge for the automotive industry (Geng et al., 2016; Praveena and Martin, 2017; Aliramezani et al., 2018).

Machine learning is being rapidly applied to a wide range of engineering and information technology problems (Bishop, 2006; Witten et al., 2016). However, employing machine learning approaches for modeling internal combustion engines has lagged behind other applications due to the existing physics-based engine and aftertreatment models (Asprion et al., 2013). The increasing engine complexity means that developing a flexible and accurate physics-based model that includes all the advanced emerging technologies has become complex requiring large amounts of effort (Thangaraja and Kannan, 2016). Trained data-driven models present a black-box approach (Yu and Li, 2001) for matching sensor outputs with inputs in a non-linear manner with no concern of physical understanding of the system components (Yusri et al., 2018; Silitonga et al., 2018). Machine learning approaches are gaining attention as an alternative for accurately predicting engine performance and emissions. This can be done regardless of the input parameters variation, if sufficient training data is available (Wong et al., 2018, 2015).

Support Vector Machine (SVM) is a popular machine learning approach that is able to generate high-precision decision boundaries based on a small subset of training data points and is capable of modelling complex and non-linear relations (Xu et al., 2013; Tanveer, 2015). The use of machine learning-based diesel emission models has been mostly limited to steady state prediction of engine emissions. Developing a simple but accurate transient emission model using an advanced machine learning technique, provides a more powerful tool for engine control, emission reduction, and on-board diagnostics. The other advantage of the proposed SVM-based model is its high convergence capability compared to the other state-of-the art approaches such as artificial neural network (ANN), or Gaussian Processes (GP)s.

A steady state diesel engine Break Mean Effective Pressure (BMEP) and NO_x emission model is developed using SVM based on the experimental data from a medium duty diesel engine. The engine speed, the amount of injected fuel and the injection rail pressure are used to model the steady state engine NO_x and BMEP. A fast response NO_x sensor is then used to carry out the transient experiments to develop and parameterize a control oriented NO_x and BMEP model.

2 Experimental Setup

A fast response electrochemical NO_x sensor (Aliramezani et al., 2019b) was mounted in the exhaust pipe of a four

cylinder medium duty Tier III diesel engine (Cummins QSB4.5 160 - Tier 3/Stage IIIA) to measure the engine transient NO_x emission. The Engine characteristics are listed in Table 1.

Table 1: Diesel engine characteristics (cum, 2019)

Engine type	In-Line, 4-Cylinder
Displacement	4.5 L
Peak BMEP	17.4 bar (@ 1500 rpm)
Aspiration	Turbocharged and Charge Air Cooled
Certification Level	Tier 3 / Stage IIIA

To read the engine main variables and operating parameters, the Cummins Engine Control Unit (ECU) is connected to a computer using J1939 connector and a hardware interface (INLINE 6). The ECU controls the Diesel engine by reading all the stock sensors mounted on the production Cummins engine including the intake manifold temperature and pressure, injection rail pressure, coolant temperature, and controlling all of the engine main actuators and operating parameters, including the injection timing(s), turbocharge boost pressure and injection amount.

The engine is tested between engine speeds of 1000 to 2500 rpm, injected fuel of 15.8 to 116.3 mg/stroke, and rail pressure between 10,000 to 20,000 bar.

3 Support Vector Machine Regression (SVM)

3.1 Model Description

Support Vector Machine (SVM) is a supervised machine learning approach used for classification and regression by producing a set of hyperplanes in an infinite-dimensional space (Drucker et al., 1997). SVM application for regression and function approximation was originally introduced by (Drucker et al., 1997). Given a set of labeled data as $\{\mathbf{u_i}, \mathbf{z_i}\}$, where $\mathbf{u_i}$ is the input and $\mathbf{z_i}$ is the target output, the optimal hyperplane, $\mathbf{y}(\mathbf{u_i})$, can be defined as:

$$\mathbf{y}(\mathbf{u_i}) = \mathbf{w}^T \mathbf{u_i} + \mathbf{b} \tag{1}$$

where, the matrix $\mathbf{w}$ and vector $\mathbf{b}$ are found by solving the SVM algorithm. For the rest of this paper, $\mathbf{y_i}$ will be used instead of $\mathbf{y}(\mathbf{u_i})$. The data set and the regression function are schematically shown in Fig. 1. As illustrated in Fig. 1, $\mathbf{y_i}$ is

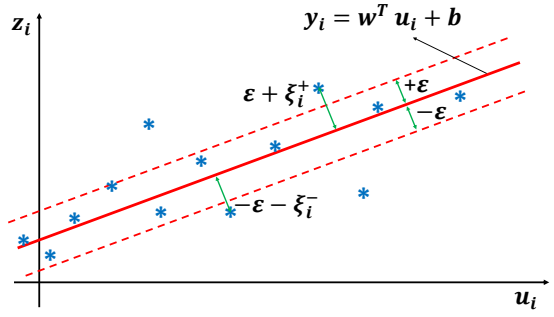

Fig. 1. SVM regression and support vectors

the predicted target, ε represents the threshold range for all the predictions, and ζ is the Slack variable (Smola and Schölkopf, 2004) added to overcome the infeasibility of the problem. In other words, the main objective is to find a prediction model for which the error $(\mathbf{y_i} - \mathbf{z_i})$ is within $(-\varepsilon, \varepsilon)$. The slack variables are considered as penalty variables to overcome the case of an infeasible optimization problem to force the error within $(-\varepsilon, \varepsilon)$. Thus, the problem can be written as the following convex optimization problem:

$$\begin{aligned} \textbf{Minimize: } & \frac{1}{2}||\mathbf{w}||_2^2 \\ \textbf{Subject to: } & \mathbf{z_i} - \mathbf{w}^T\mathbf{u_i} - \mathbf{b} \leq \varepsilon \\ & \mathbf{w}^T\mathbf{u_i} + \mathbf{b} - \mathbf{z_i} \leq -\varepsilon \end{aligned} \tag{2}$$

In other words, the $\mathbf{y}(\mathbf{u})$ exists such that there are some ε for which the prediction based on data set $(\mathbf{u_i}, \mathbf{z_i})$ is within ε distance from the target training points. The ε-insensitive linear loss function is defined as (Vapnik, 2013):

$$L_\varepsilon(\mathbf{z_i}, \mathbf{y_i}) = \begin{cases} 0 & |\mathbf{z_i} - \mathbf{y_i}| \leq \varepsilon \\ |\mathbf{z_i} - \mathbf{y_i}| - \varepsilon & \text{otherwise} \end{cases} \tag{3}$$

to consider the fact that if the training error is less than ε, the loss function would be equal to zero. Thus, the problem of finding $\mathbf{w}$ and $\mathbf{b}$ is changed to the problem of minimizing the empirical risk function (Smola and Schölkopf, 2004):

$$R_{emp}(\mathbf{w}, \mathbf{b}) = \frac{1}{N}\sum_{i=1}^{N} L_\varepsilon(\mathbf{z_i}, \mathbf{y_i}) \tag{4}$$

and $\frac{1}{2}\langle \mathbf{w}, \mathbf{w} \rangle$ (the inner product) simultaneously.

The final objective is to keep the training error $(\mathbf{z_i} - \mathbf{y_i})$ within $(-\varepsilon, \varepsilon)$:

$$-\varepsilon \leq \mathbf{z_i} - \mathbf{y_i} \leq \varepsilon \tag{5}$$

The slack variables ζ_i^+ and ζ_i^- are added to the optimization problem to overcome infeasible constraints for the other training points (Smola and Schölkopf, 2004):

$$-\varepsilon - \zeta_i^- \leq \mathbf{z_i} - \mathbf{y_i} \leq \varepsilon + \zeta_i^+ \tag{6}$$

It can be proven that $\zeta_i^- + \zeta_i^+$ is equal to the loss function $(L_\varepsilon(\mathbf{z_i}, \mathbf{y_i}))$ defined in Eqn. (3). Also, at least one of the slack variables must have zero value $(\zeta_i^- \zeta_i^+ = 0)$. The loss function is depicted schematically in Fig. 2. The empirical risk function

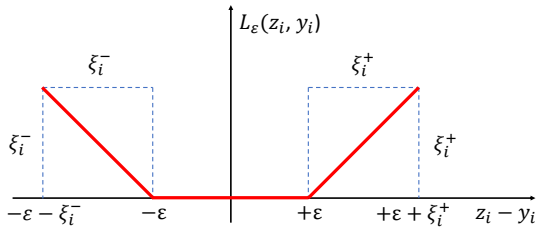

Fig. 2. $\varepsilon-$sensitive Loss function with slack variable based on the (Vapnik, 2013)

can be rewritten using on the slack variables as:

$$R_{emp}(\mathbf{w}, \mathbf{b}) = \frac{1}{N}\sum_{i=1}^{N} \left(\zeta_i^- + \zeta_i^+\right) \tag{7}$$

Then, the optimization problem can be changed to minimize the empirical risk function defined in Eq. (7) and $\frac{1}{2}||\mathbf{w}||_2^2$ simultaneously. Using Equations (7) and (6), the optimization problem can be summarized as follow:

$$\begin{aligned} \textbf{Minimize:}\quad & \frac{1}{2}||\mathbf{w}||_2^2 + C\sum_{i=1}^{N}\left(\zeta_i^- + \zeta_i^+\right) \\ \textbf{Subject to:}\quad & -\mathbf{z_i} + \mathbf{y_i} + \varepsilon + \zeta_i^+ \geq 0 \\ & \mathbf{z_i} - \mathbf{y_i} + \varepsilon + \zeta_i^- \geq 0 \\ & \zeta_i^- \geq 0, \quad \zeta_i^+ \geq 0 \end{aligned} \tag{8}$$

The primary objective function is now defined based on Eq. (8) as (Smola and Schölkopf, 2004):

$$\begin{aligned} L = & \frac{1}{2}||\mathbf{w}||_2^2 + C\sum_{i=1}^{N}\left(\zeta_i^- + \zeta_i^+\right) \\ & - \sum_{i=1}^{N}\alpha_i^+(-\mathbf{z_i} + \mathbf{y_i} + \varepsilon + \zeta_i^+) - \sum_{i=1}^{N}\mu_i^+\zeta_i^+ \\ & - \sum_{i=1}^{N}\alpha_i^-(\mathbf{z_i} - \mathbf{y_i} + \varepsilon + \zeta_i^-) - \sum_{i=1}^{N}\mu_i^-\zeta_i^- \end{aligned} \tag{9}$$

where L is the Lagrangian function and α_i^+, α_i^-, μ_i^+, and μ_i^- are Lagrangian Multipliers all of which are greater than or equal to zero. The objective is to minimize Eq. (9) by adjusting the optimization variables $\mathbf{w}$, $\mathbf{b}$, ζ_i^+, and ζ_i^-. Differentiating the Lagrangian with respect to these variables (Smola and Schölkopf, 2004) and setting to zero:

$$\frac{\partial L}{\partial \mathbf{w}} = 0 \;\rightarrow\; w = \sum_{i=1}^{N}(\alpha_i^+ - \alpha_i^-)\mathbf{u_i} \tag{10a}$$

$$\frac{\partial L}{\partial \mathbf{b}} = 0 \;\rightarrow\; \sum_{i=1}^{N}(\alpha_i^+ - \alpha_i^-) = 0 \tag{10b}$$

$$\frac{\partial L}{\partial \zeta_i^+} = 0 \;\rightarrow\; \alpha_i^+ + \mu_i^+ = C \tag{10c}$$

$$\frac{\partial L}{\partial \zeta_i^-} = 0 \;\rightarrow\; \alpha_i^- + \mu_i^- = C \tag{10d}$$

where Eq. (10a) is the support vector expansion, Eq. (10b) contains the bias constraints while Eq. (10c), and Eq. (10d) include the box constraints, and C is the regularization parameter used to trade-off between minimizing the training error and maximizing the prediction smoothness. Examining Eq. (10a), $\mathbf{w}$ is exclusively dependant on the linear combination of training inputs $\mathbf{u_i}$. Combining Eqs. (10a)-(10d) with Eq. (9), the dual optimization problem is obtained as the following standard Quadratic programming form (QP)(Bellman et al., 1954):

$$\begin{aligned} \textbf{Minimize:}\quad & \frac{1}{2}\alpha^T\mathscr{H}\alpha + f^T\alpha \\ \textbf{Subject to:}\quad & A_{eq}\alpha = B_{eq} \end{aligned} \tag{11}$$

where

$$\alpha = \begin{bmatrix} \alpha^+ \\ \alpha^- \end{bmatrix},\quad \mathscr{H} = \begin{bmatrix} H & -H \\ -H & H \end{bmatrix},\quad \mathbf{f} = \begin{bmatrix} -\mathbf{z_i} + \varepsilon \\ \mathbf{z_i} + \varepsilon \end{bmatrix},$$
$$H = \begin{bmatrix} \mathbf{u_i}^T\ \mathbf{u_j} \end{bmatrix},\quad \mathbf{A_{eq}} = [1 \ldots 1 \quad -1 \ldots -1],\quad \mathbf{B_{eq}} = [0] \tag{12}$$

$\mathbf{w}$ can be calculated by finding α (Solving Eq. (12)) and substituting it into Eq. (10a).

Karush-Kuhn-Tucker (KKT) (Karush, 1939; Kuhn and Tucker, 1951) approach is used to find $\mathbf{b}$ which requires all the following equations to be fulfilled at the optimum point:

$$\alpha_i^+(-\mathbf{z_i} + \mathbf{y_i} + \varepsilon + \zeta_i^+) = 0 \tag{13a}$$

$$\alpha_i^-(\mathbf{z_i} - \mathbf{y_i} + \varepsilon + \zeta_i^-) = 0 \tag{13b}$$

$$\mu_i^+\zeta_i^+ = (C - \alpha_i^+)\zeta_i^+ \tag{13c}$$

$$\mu_i^-\zeta_i^- = (C - \alpha_i^-)\zeta_i^- \tag{13d}$$

Considering KKT conditions listed in Eq. (13), only the following five possible cases can take place:

$$\alpha_i^+ = \alpha_i^- = 0 \tag{14a}$$

$$0 < \alpha_i^+ < C,\ \alpha_i^- = 0 \tag{14b}$$

$$0 < \alpha_i^- < C,\ \alpha_i^+ = 0 \tag{14c}$$

$$\alpha_i^+ = C,\ \alpha_i^- = 0 \tag{14d}$$

$$\alpha_i^- = C,\ \alpha_i^+ = 0 \tag{14e}$$

For point i to lie on the support vectors, $\mathbf{z_i} - \mathbf{y_i}$ must be exactly equals to ε or $-\varepsilon$. Therefore, the only acceptable conditions are Eqs. (14b) and (14c). Then, the support vectors set, S, can be defined as:

$$S = \{\, i \mid 0 < \alpha_i^+ + \alpha_i^+ < C\} \tag{15}$$

Over the support vectors set, we have:

$$\mathbf{z_i} = \mathbf{y_i} + sign(\alpha_i^+ - \alpha_i^-)\varepsilon \quad i \in S \tag{16}$$

where $\mathbf{b}$ can be found by solving Eq. (16) as:

$$\mathbf{b} = \frac{1}{|S|}\sum_{i\in S}^{S}(\mathbf{z_i} - \mathbf{w}^T\mathbf{u_i} - sign(\alpha_i^+ - \alpha_i^-)\varepsilon) \tag{17}$$

The block diagram of the SVM regression is shown in Fig. 3.

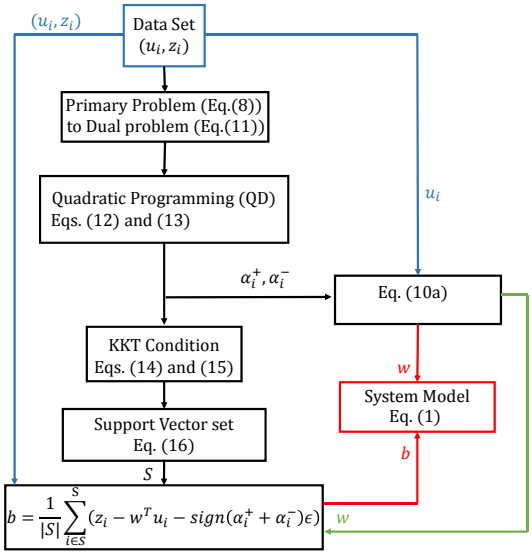

Fig. 3. SVM Model training schematic

3.2 NO_x *and* BMEP *Steady State Model*

In this section, a steady state model of diesel engine NO_x emission and BMEP is developed based on the SVM algorithm explained above and following Fig. 3. Based on the experimental

results of steady state engine operation at different operating conditions are collected ($\mathbf{u_i}$, $\mathbf{z_i}$). The NO_x emission and *BMEP* are modeled as a function of injected fuel amount, fuel rail pressure, and engine speed. The model features are selected based on a polynomial function proposed in (Alirameza ni et al., 2019a) which includes the most significant factors affecting NOx emission that were available for measurement in this experiment. The SVM regression model for steady state NO_x and *BMEP* is then defined as:

$$\mathbf{y_{ss}} = \mathbf{w}^T u + \mathbf{b} \tag{18}$$

where

$$\mathbf{y_{ss}} = \begin{bmatrix} NO_{x,ss} \\ BMEP_{ss} \end{bmatrix}, \ \mathbf{b} = \begin{bmatrix} 465.32 \\ 9.4873 \end{bmatrix},$$

$$\mathbf{w} = \begin{bmatrix} 735.90 & 8.6806 \\ -1472.2 & 0.2434 \\ 680.00 & -3.8273 \\ -983.40 & -3.1383 \\ 1171.0 & -1.0818 \\ -574.4 & 4.3550 \\ 560.30 & 2.5611 \end{bmatrix}, \ u = \begin{bmatrix} \mathrm{m}_f \\ \mathrm{n} \\ \mathrm{p}_r \\ \mathrm{m}_f^2 \\ \mathrm{n}^2 \\ \mathrm{p}_r^2 \\ \mathrm{m}_f^3 \end{bmatrix} \tag{19}$$

in which, m_f is the injected fuel amount ($mg/stroke$), n is engine speed (rpm), p_r is fuel rail pressure (bar), $NO_{x,ss}$ is the steady state NO_x concentration (ppm), and $BMEP_{ss}$ is the steady state value of BMEP.

Steady state engine NO_x emission and BMEP results are used to train the SVM model for BMEP and NO_x. The SVM training parameter ε is selected based on the error tolerance and the regularization vector C and is selected to be high enough to capture all of the model features. As illustrated in Fig. 4, the squared correlation coefficient, R^2 increases by increasing C and it plateaus after a specific C value. The vector C parameters are selected to be two times of the corresponding C value of the plateaued R^2 vs C curve. The selected $\mathbf{C}$ and ε vectors are as follows:

$$\mathbf{C} = \begin{bmatrix} C_{NOx} \\ C_{BMEP} \end{bmatrix} = \begin{bmatrix} 50000 \\ 5000 \end{bmatrix}, \ \varepsilon = \begin{bmatrix} \varepsilon_{NOx} \\ \varepsilon_{BMEP} \end{bmatrix} = \begin{bmatrix} 10 \\ 0.2 \end{bmatrix} \tag{20}$$

The experimental vs trained BMEP and NO_x models are shown in Figure 5 along with the corresponding support vectors. Both BMEP and NO_x models were capable of accurately predicting the steady state BMEP and NO_x with correlation coefficient, R^2, of 0.999 and 0.966 respectively. The cost function vs iteration for BMEP and NO_x are shown in Figure 6 and both depict the quick convergence of the optimization using the SVM quadratic programming algorithm.

4 Nonlinear Control Oriented Model (NCOM)

The steady state model defined above is now augmented with a simple transient model. The discrete time control oriented model of NO_x concentration at step k at a sampling interval of T, is calculated as:

$$NO_x(k) = (1 - \frac{T}{\tau_{NOx} + T})NO_x(k-1) + \frac{T}{\tau_{NOx} + T} NO_{x,ss}(k) \tag{21}$$

and the BMEP at step k is calculated as:

$$BMEP(k) = (1 - \frac{T}{\tau_{BMEP} + T})BMEP(k-1) + \frac{T}{\tau_{BMEP} + T} BMEP_{ss}(k) \tag{22}$$

where $NO_{x,ss}(k)$ and $BMEP_{ss}(k)$ are the steady state NO_x and BMEP calculated using SVM in Eqn. (19) while τ_{NOx} and τ_{BMEP} are approximated as linear first order time constants for NO_x and BMEP respectively which are estimated based on the experimental data and are found to be 1 seconds and 0.2 seconds respectively Alirameza ni et al. (2019a). This study aims to model the engine transients using a simple structure and a first order lag for BMEP and NO_x which is found to be sufficiently precise for future control algorithms.

The model inputs, states, parameters and outputs are classified as vectors. The vector $\mathbf{x}$ contains two model states:

$$\mathbf{x(k)} = [NO_x(k) \ \ BMEP(k)] \tag{23}$$

Based on (Alirameza ni et al., 2019a), the vector $\mathbf{u}$ contains model inputs using Eq. (19):

$$\mathbf{u(k)} = [m_f(k) \ \ n(k) \ \ p_r(k) \ \ m_f^2(k) \ \ n^2(k) \ \ p_r^2(k) \ \ m_f^3(k)] \tag{24}$$

With x_1 and x_2 from Eqn (23), the vector $\mathbf{y}$ contains two model outputs:

$$\mathbf{y(k)} = [x_1(k) \ \ x_2(k)] \tag{25}$$

Combining Eqs. (18) to (25) results in:

$$\mathbf{x}(k) = \mathbf{A}\mathbf{x}(k-1) + \mathbf{B}\mathbf{u}^{'}(\mathbf{k-1}) \tag{26}$$

where matrices $\mathbf{A}$, $\mathbf{B}^{'}$, $\mathbf{B}$ and $\mathbf{u}^{'}$(k) are:

$$\mathbf{A} = \begin{bmatrix} 1 - \frac{T}{\tau_{NOx}+T} & 0 \\ 0 & 1 - \frac{T}{\tau_{BMEP}+T} \end{bmatrix}$$

$$\mathbf{B} = \begin{bmatrix} \frac{T}{\tau_{NOx}+T} & 0 \\ 0 & \frac{T}{\tau_{BMEP}+T} \end{bmatrix} \tag{27}$$

$$\mathbf{u}^{'}(\mathbf{k}) = \mathbf{w}^T \mathbf{u}(k) + b$$

To validate the trained BMEP and NO_x models, the transient behavior of the proposed control-oriented model is then examined for step changes of injected fuel and rail pressure and the results are shown in Figure 7. The control-oriented model provides a precise representation of the system output dynamics, NO_x and BMEP, with root mean square error (RMS) of 10 (ppm) and 0.26 (bar) for NO_x and BMEP respectively. Implementing the SVM algorithm has reduced the RMS with respect to a similar model but trained with a trust-region algorithm (Alirameza ni et al., 2019a) by 0.12 (bar) and 22.8 (ppm) for BMEP and NO_x respectively.

5 Conclusions

A support vector machine (SVM) approach is implemented to predict the steady state NO_x and BMEP of a medium duty diesel engine. The SVM model was first trained using the steady state experimental data. The engine speed, the amount

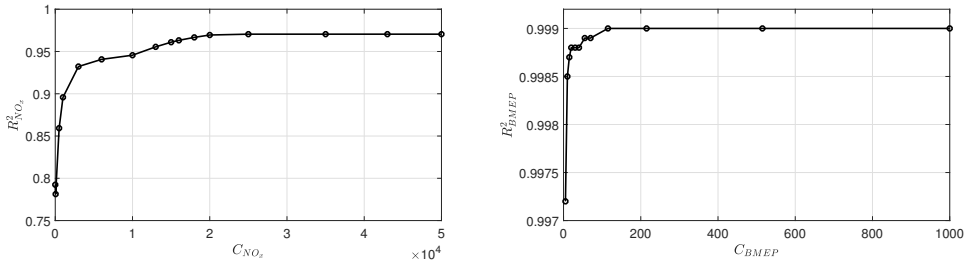

Fig. 4. Coefficient of correlation vs regularization parameter, C, for NO_x and BMEP

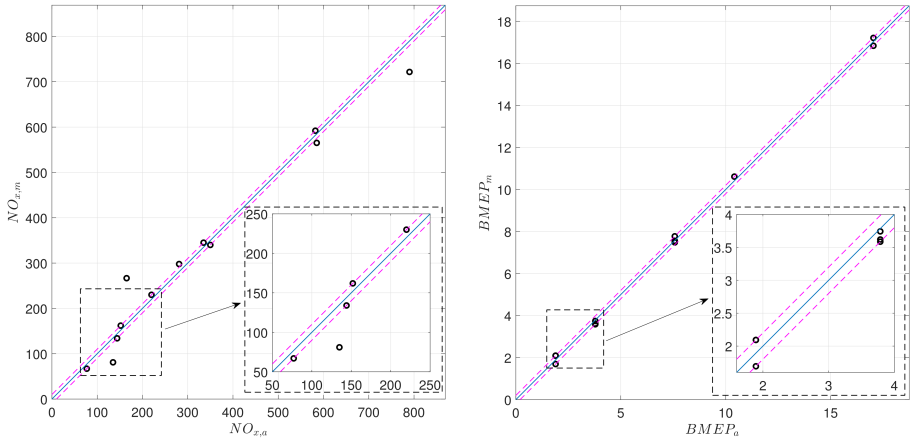

Fig. 5. SVM model prediction Vs Experiments for BMEP and NO_x

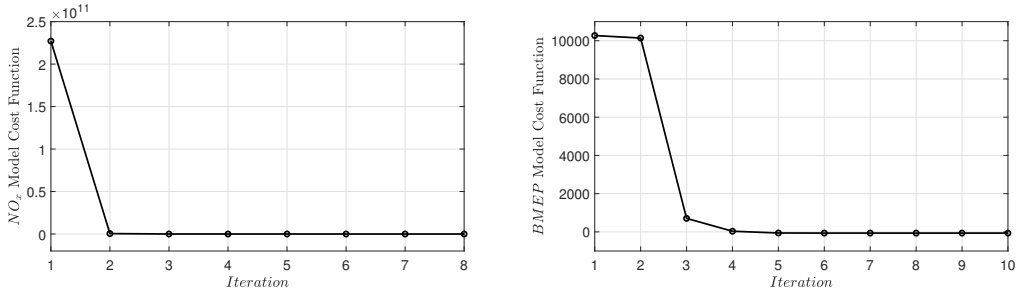

Fig. 6. Cost Function Vs iteration for BMEP and NO_x

of injected fuel and the injection rail pressure are used to predict the steady state engine NO_x emission and BMEP.

A control oriented model was then developed based on the SVM model to predict the transient behavior of the system. A fast response electrochemical NO_x sensor is used to verify the transient response of the control oriented model for different steps of injected fuel and rail pressure. The results show that the SVM algorithm is capable of accurately predicting the NO_x and BMEP in steady state and transient conditions. The RMS error for the NO_x and BMEP transient test were 10 ppm and 0.26 bar respectively.

In future work, the proposed model will be extended to also include other important engine emissions such as unburned hydrocarbons. This will provide a powerful comprehensive tool for overall emission reduction and transient emissions trade-off. In addition, this model can be used to develop different types of model-based engine control strategies, such as model predictive control for observer design and model-based fault detection and isolation (FDI).

References

(2019). www.cummins.com/engines.

Aliramezani, M., Koch, C., and Patrick, R. (2018). Phenomenological model of a solid electrolyte NOx and O2 sensor using temperature perturbation for on-board diagnostics. *Solid State Ionics*, 321, 62 – 68.

Aliramezani, M., Norouzi, A., Koch, C.R., and Hayes, R.E. (2019a). A control oriented diesel engine NOx emission model for on board diagnostics and engine control with sensor feedback. In *Proceedings of Combustion Institute - Canadian Section (CICS)*.

Aliramezani, M., Koch, C.R., Secanell, M., Hayes, R.E., and Patrick, R. (2019b). An electrochemical model of an amperometric NOx sensor. *Sensors and Actuators B: Chemical*, 290, 302 – 311.

Asprion, J., Chinellato, O., and Guzzella, L. (2013). A fast and accurate physics-based model for the NOx emissions of Diesel engines. *Applied Energy*, 103, 221 – 233.

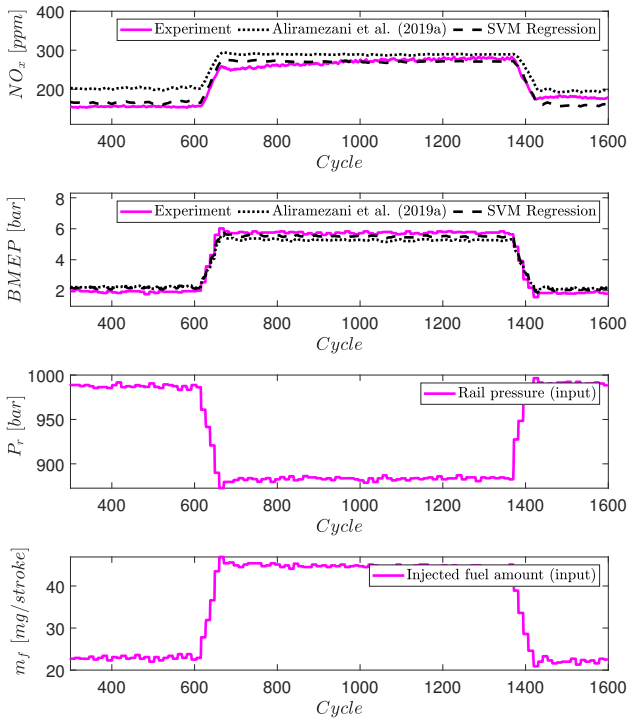

Fig. 7. Experiment vs Trust-region Algorithm vs Support Vector Machine

Bari, S. and Hossain, S.N. (2013). Waste heat recovery from a diesel engine using shell and tube heat exchanger. *Applied Thermal Engineering*, 61(2), 355 – 363.

Bellman, R. et al. (1954). The theory of dynamic programming. *Bulletin of the American Mathematical Society*, 60(6), 503–515.

Bishop, C.M. (2006). *Pattern recognition and machine learning*. springer.

Dasappa, S. and Sridhar, H.V. (2013). Performance of a diesel engine in a dual fuel mode using producer gas for electricity power generation. *International Journal of Sustainable Energy*, 32(3), 153–168.

Dhar, A. and Agarwal, A.K. (2014). Performance, emissions and combustion characteristics of karanja biodiesel in a transportation engine. *Fuel*, 119, 70 – 80.

Drucker, H., Burges, C.J., Kaufman, L., Smola, A.J., and Vapnik, V. (1997). Support vector regression machines. In *Advances in neural information processing systems*, 155–161.

Geng, P., Tan, Q., Zhang, C., Wei, L., He, X., Cao, E., and Jiang, K. (2016). Experimental investigation on NOx and green house gas emissions from a marine auxiliary diesel engine using ultralow sulfur light fuel. *Science of The Total Environment*, 572(Supplement C), 467 – 475.

Karush, W. (1939). Minima of functions of several variables with inequalities as side constraints. *M. Sc. Dissertation. Dept. of Mathematics, Univ. of Chicago*.

Kuhn, H.W. and Tucker, A.W. (1951). Nonlinear programming, in (J. Neyman, ed.) Proceedings of the Second Berkeley Symposium on Mathematical Statistics and Probability.

Pali, H.S., Kumar, N., and Alhassan, Y. (2015). Performance and emission characteristics of an agricultural diesel engine fueled with blends of sal methyl esters and diesel. *Energy Conversion and Management*, 90, 146 – 153.

Praveena, V. and Martin, M. (2017). A review on various after treatment techniques to reduce NOx emissions in a CI engine. *Journal of the Energy Institute*.

Pronk, A., Coble, J., and Stewart, P.A. (2009). Occupational exposure to diesel engine exhaust: a literature review. *Journal of exposure science and environmental epidemiology*, 19(5), 443.

Silitonga, A., Masjuki, H., Ong, H.C., Sebayang, A., Dharma, S., Kusumo, F., Siswantoro, J., Milano, J., Daud, K., Mahlia, T., Chen, W.H., and Sugiyanto, B. (2018). Evaluation of the engine performance and exhaust emissions of biodiesel-bioethanol-diesel blends using kernel-based extreme learning machine. *Energy*, 159, 1075 – 1087.

Smola, A.J. and Schölkopf, B. (2004). A tutorial on support vector regression. *Statistics and computing*, 14(3), 199–222.

Tan, Y.H., Abdullah, M.O., Nolasco-Hipolito, C., Zauzi, N.S.A., and Abdullah, G.W. (2017). Engine performance and emissions characteristics of a diesel engine fueled with diesel-biodiesel-bioethanol emulsions. *Energy Conversion and Management*, 132, 54 – 64.

Tanveer, M. (2015). Robust and sparse linear programming twin support vector machines. *Cognitive Computation*, 7(1), 137–149.

Thangaraja, J. and Kannan, C. (2016). Effect of exhaust gas recirculation on advanced diesel combustion and alternate fuels - a review. *Applied Energy*, 180, 169 – 184.

Vapnik, V. (2013). *The nature of statistical learning theory*. Springer science & business media.

Witten, I.H., Frank, E., Hall, M.A., and Pal, C.J. (2016). *Data Mining: Practical machine learning tools and techniques*. Morgan Kaufmann.

Wong, P.K., Gao, X.H., Wong, K.I., and Vong, C.M. (2018). Online extreme learning machine based modeling and optimization for point-by-point engine calibration. *Neurocomputing*, 277, 187–197.

Wong, P.K., Wong, K.I., Vong, C.M., and Cheung, C.S. (2015). Modeling and optimization of biodiesel engine performance using kernel-based extreme learning machine and cuckoo search. *Renewable Energy*, 74, 640 – 647.

Xu, Y., Guo, R., and Wang, L. (2013). A twin multi-class classification support vector machine. *Cognitive computation*, 5(4), 580–588.

Yadav, A.K., Khan, M.E., Dubey, A.M., and Pal, A. (2016). Performance and emission characteristics of a transportation diesel engine operated with non-edible vegetable oils biodiesel. *Case Studies in Thermal Engineering*, 8, 236 – 244.

Yu, W. and Li, X. (2001). Some new results on system identification with dynamic neural networks. *IEEE Transactions on Neural Networks*, 12(2), 412–417.

Yusri, I., Majeed, A.A., Mamat, R., Ghazali, M., Awad, O.I., and Azmi, W. (2018). A review on the application of response surface method and artificial neural network in engine performance and exhaust emissions characteristics in alternative fuel. *Renewable and Sustainable Energy Reviews*, 90, 665 – 686.